and C), while confining the influence of the El Niño-Southern Oscillation (ENSO) (*28*, *29*) to the interannual time scale (Fig. 4, E and F).

The semi-arid Sahel emerges as a region highly sensitive to SST variability in all tropical basins, remote (Pacific) and local (Atlantic and Indian). A positive trend in equatorial Indian Ocean SSTs, between East Africa and Indonesia, is identified as the proximate cause for the negative rainfall trend observed in the Sahel from the late 1960s to the 1980s (Fig. 4, A and B). Teaming up with an occasionally warmer-than-average eastern equatorial Atlantic Ocean (*15*, *16*), it formed a low-latitude ring of warm SSTs around Africa that may have disrupted the fragile balance that defines the monsoon, between the competing effects of high summertime land surface temperatures and the associated development of a land-ocean temperature contrast versus the availability of moisture (*30*). Rainfall anomalies of opposite sign across the Sahel and in the equatorial Indian Ocean (Fig. 4C) support the hypothesis that the oceanic warming around Africa may indeed have weakened the land-ocean temperature contrast and consequently the monsoon, causing deep convection to migrate over the ocean and engendering widespread drought over land, from the Atlantic coast of West Africa to the highlands of Ethiopia.

References and Notes

1. S. E. Nicholson, *Mon. Weather Rev.* **108**, 473 (1980).
2. M. H. Glantz, R. W. Katz, *Ambio* **14** (no. 6), 334 (1985).
3. J. G. Charney, *Q. J. R. Meteorol. Soc.* **101**, 193 (1975).
4. The albedo-precipitation feedback popularized by Charney was first proposed by J. Otterman [*Science* **186**, 531 (1974)].
5. Y. C. Sud, M. Fennessy, *J. Clim.* **2**, 105 (1982).
6. Y. Xue, J. Shukla, *J. Clim.* **6**, 2232 (1993).
7. C. M. Taylor, E. F. Lambin, N. Stephenne, R. J. Harding, R. L. H. Essery, *J. Clim.* **15**, 3615 (2002).
8. J. Fairhead, M. Leach, *Deforestation: Global analyses and local realities — studies in West Africa* (Routledge, London, 1998).
9. E. F. Lambin *et al.*, *Global Environ. Change* **11**, 261 (2001).
10. K. Rasmussen *et al.*, *Global Environ. Change* **11**, 271 (2001).
11. C. J. Tucker, H. E. Dregne, W. W. Newcomb, *Science* **253**, 299 (1991).
12. C. K. Folland, T. N. Palmer, D. E. Parker, *Nature* **320**, 602 (1986).
13. T. N. Palmer, *Nature* **322**, 251 (1986).
14. D. P. Rowell, C. K. Folland, K. Maskell, M. N. Ward, *Q. J. R. Meteorol. Soc.* **121**, 669 (1995).
15. S. Hastenrath, P. J. Lamb, *Mon. Weather Rev.* **105**, 1019 (1977).
16. P. J. Lamb, *Mon. Weather Rev.* **106**, 482 (1978).
17. B. Fontaine, S. Janicot, *J. Clim.* **9**, 2935 (1996).
18. NSIPP1, as described in abstract. J. T. Bacmeister, P. J. Pegion, S. D. Schubert, M. J. Suarez, *NASA Technical Memo.* **104606**, vol. 17 (2000). Available at http://nsipp.gsfc.nasa.gov.
19. SSTs from three different data sets were used to force the ensemble of atmospheric general circulation model (ACGM) integrations over the sub-periods 1930–48, 1949–81, and 1982–2000. The data sets are (i) the Hadley Centre product (*31*), (ii) the GISST product (*32*), and (iii) the "Reynolds" product (*33*). The temporal discontinuities in boundary conditions were found to be of no consequence to the analysis presented here: the regression pattern of Fig. 2F was recalculated using the Hadley Centre data set from 1930 to 1999 and found to be identical to the one presented here, calculated using the boundary condition data set. Also, projections of the same regression pattern onto the Hadley Centre product and onto the boundary condition data set were found to correlate at 0.97 when care was taken to exclude gridpoints south of 50°S.
20. R. S. Vose *et al.*, *The Global Historical Climatology Network: Long-term monthly temperature, precipitation, sea level pressure, and station pressure data*. ORNL/CDIAC-53, NDP-041 (Carbon Dioxide Information Analysis Center, Oak Ridge National Laboratory, Oak Ridge, TN, 1992).
21. PCA is a mathematical procedure routinely used in the geophysical sciences to extract the dominant patterns of variability. It identifies the spatial structures, or empirical orthogonal functions (EOFs), and related temporal structures, also known as PCs, that sequentially maximize the fraction of the total variability that they represent (*34–36*).
22. A. Giannini, R. Saravanan, P. Chang, data not shown.
23. The impact of tropical Atlantic SST anomalies on the West African monsoon has been the subject of observational studies dating back to the 1970s (*15*, *16*), as well as of two recent modeling studies by Vizy and Cook (*37*, *38*). In the presence of an equatorial Atlantic SST anomaly akin to the one associated with the model's Gulf of Guinea PC (Fig. 2C), a dipole in precipitation stands out in observations, with anomalies of opposite sign in the Sahel and along the Gulf of Guinea coast. This dipole is captured in our analysis of observed rainfall variability in the Sahel EOF (*22*); the regression of the observed Sahel PC onto SST (*22*) does bear the association out, with significant regression anomalies in the equatorial Atlantic, as well as in the rest of the tropical oceans. PCA of model output, in contrast, though separating rainfall variability in the Sahel from rainfall variability along the Gulf of Guinea coast (Fig. 2, A and D) in the two leading EOFs also decouples the association between eastern equatorial Atlantic SSTs and the rainfall dipole. AGCMs, thus far, have not been able to capture the dipole in precipitation, and the model analyzed here is no exception. Whether this model's failure to explicitly represent the dipole in precipitation is a dynamical limitation of the model, an artifact of PCA, or the expression of a substantial dynamical difference between Sahel and Gulf of Guinea precipitation, remains to be seen.
24. K. H. Cook, *J. Clim.* **7**, 400 (1994).
25. Interannual SST variability is disabled in a 160-year long integration by substituting the observed record of SST with monthly climatology. Land-atmosphere interaction is disabled in a single integration forced with the observed record of SST over 1950−1999 by fixing evaporation efficiencies to monthly climatology, as computed from the ensemble of integrations. For details on the method, see (*39*, *40*).
26. An interactive vegetation, in addition to the interactive land surface, could further amplify the ocean-forced signal, as in the intermediate complexity model of N. Zeng, J. D. Neelin, K.-M. Lau and C. J. Tucker [*Science* **286**, 1537 (1999)]. Such an amplification could at least partially account for the difference in magnitude between observed and modeled rainfall variability (Fig. 1).
27. M. N. Ward, *J. Clim.* **11**, 3167 (1998).
28. S. Janicot, A. Harzallah, B. Fontaine, V. Moron, *J. Clim.* **11**, 1874 (1998).
29. J. C. H. Chiang, A. H. Sobel, *J. Clim.* **15**, 2616 (2002).
30. C. Chou, J. D. Neelin, H. Su, *Q. J. R. Meteorol. Soc.* **127**, 1869 (2001).
31. N. A. Rayner *et al.*, in press.
32. N. A. Rayner, E. B. Horton, D. E. Parker, C. K. Folland, R. B. Hackett, *Climate Research Technical Note* **74** (1996). Available at: www.met-office.gov.uk/research/hadleycentre/obsdata/GISST.html
33. W. R. Reynolds, T. M. Smith., *J. Clim.* **7**, 929 (1994).
34. R. W. Preisendorfer, *Principal Component Analysis in Meteorology and Oceanography*, C. Mobley, Ed. (Elsevier, Amsterdam, 1988).
35. H. von Storch, F. W. Zwiers, *Statistical Analysis in Climate Research* (Cambridge Univ. Press, Cambridge, 1999).
36. J. P. Peixoto, A. H. Oort, *Physics of Climate* (American Institute of Physics, New York, 1992), appendix B.
37. E. K. Vizy, K. H. Cook, *J. Clim.* **14**, 795 (2001).
38. E. K. Vizy, K. H. Cook, *J. Geophys. Res.* **107(D3)**, doi: 10.1029/2001JD000686 (2002).
39. R. D. Koster, M. J. Suarez, *J. Geophys. Res.* **100(D7)**, 13775 (1995).
40. R. D. Koster, M. J. Suarez, M. Heiser, *J. Hydrometeorol.* **1**, 26 (2000).
41. We acknowledge the scientific advice and technical support provided by M. Suarez and the NSIPP Team at NASA/GSFC (M. Rienecker, J. Bacmeister, M. Kistler, S. Schubert, P. Pegion, and N. Johnson). Supported in part by NASA InterAgency agreement W-19,750. The National Center for Atmospheric Research is operated by the University Corporation for Atmospheric Research under sponsorship of NSF.

Increased Longevities of Post-Paleozoic Marine Genera After Mass Extinctions

Arnold I. Miller[1]* and Michael Foote[2]

Cohorts of marine taxa that originated during recoveries from mass extinctions were commonly more widespread spatially than those originating at other times. Coupled with the recognition of a correlation between the geographic ranges and temporal longevities of marine taxa, this observation predicts that recovery taxa were unusually long-lived geologically. We analyzed this possibility by assessing the longevities of marine genus cohorts that originated in successive substages throughout the Phanerozoic. Results confirm that several mass extinction recovery cohorts were significantly longer lived than other cohorts, but this effect was limited to the post-Paleozoic, suggesting differences in the dynamics of Paleozoic versus post-Paleozoic diversification.

In evaluating the global biotic effects of mass extinctions, attention has focused increasingly on recovery biotas, the taxa that originated or contributed to diversity in the immediate aftermaths of extinction events (*1–5*). Postextinction diversification has proven to be more geographically and temporally complex than once envisioned, with the onset of major rebounds in diversity characterized by lag times and geographic variability (*6–9*). Nevertheless, several principles

have emerged regarding the biological attributes of recovery taxa. They are thought to be characterized by geographic and/or environmental (i.e., spatial) distributions that were substantially broader, on average, than those of taxa originating at other times (4, 10), although this has not been demonstrated definitively for all of the major mass extinctions of the Phanerozoic. In addition, macroevolutionary theory suggests that taxa with broad spatial distributions should persist for longer geological intervals than those with narrow distributions (11, 12). Thus, it can be hypothesized that cohorts of taxa originating immediately after mass extinctions exhibited significantly greater longevities than their counterparts that originated in surrounding intervals. Here, we demonstrate that this was, indeed, the case for several post-Paleozoic recovery cohorts and that the pattern is impervious to several plausible artifacts. Interestingly, the pattern does not extend back to recovery cohorts of the Paleozoic era.

The analyses were conducted with Sepkoski's genus-level marine compendium (13), a robust resource for the investigation of large-scale patterns of diversification and extinction (14). Sepkoski's "substage"-level stratigraphic binning was maintained for the present study, and only genera whose first and last appearances were resolved to the levels of these substage bins were included here (15). The longevity of each genus was calibrated as the number of bins for which it was extant.

Figure 1A depicts the mean longevities of cohorts originating in Phanerozoic intervals ranging from the late Vendian through the Quaternary. Of particular note are three statistically significant (15) longevity maxima in the post-Paleozoic that correspond to the Early Induan and Late Induan of the Early Triassic; the Late Norian of the latest Triassic and the adjacent Hettangian of the earliest Jurassic; and the Early Berriasian of the Early Cretaceous (16). In addition, although not as pronounced as the earlier maxima, a local maximum is observed for the Early Paleocene (supporting online text).

A comparison of mean genus longevities with Phanerozoic genus extinction rates (17) suggests a close relation between longevity maxima and mass extinctions (Fig. 1B). Three of the maxima encompass intervals immediately after three of the "big five" mass extinctions of the Phanerozoic: the Late Permian, Late Triassic, and Late Cretaceous (K/T) events. In addition, the Early Berriasian maximum occurs immediately after an interval of ele-

vated extinction (18) in the Late Tithonian.

Before considering the possible biological importance of the observed signal, it is necessary to assess potential nonbiological factors that might have played artifactual roles in producing the outcome. First, a decline analogous to that exhibited in the approach to the

Recent might also have been produced in the approach to any major extinction event (supporting online text). To assess this possibility, the analysis was redone after culling all genera that became extinct during the mass extinctions in question, as well as during additional post-Paleozoic extinction events (15).
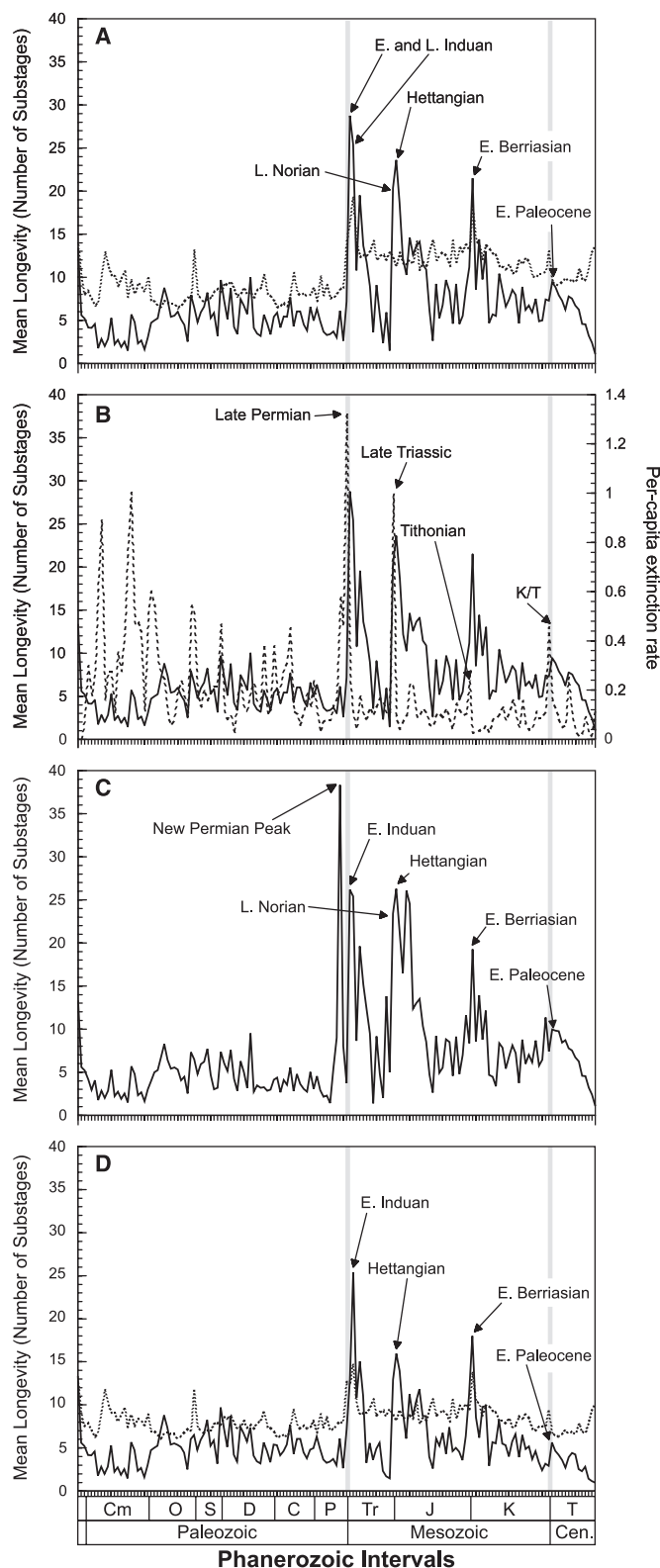

Fig. 1. Mean longevities of genus cohorts originating throughout the Phanerozoic and latest Neoproterozoic (solid lines). (**A**) Maxima are labeled; statistical significance is indicated when the peak exceeds the upper 95% confidence interval (dotted line) derived with a randomization procedure (15). (**B**) Mean genus longevities compared with per capita extinction rates (dotted line). Extinction peaks that precede longevity maxima are labeled. (**C**) The pattern after culling genera that became extinct during several post-Paleozoic mass extinctions (18). (**D**) The pattern after culling genera that survived to the present day; dotted line as in (A) but based only on genera that did not survive to the present day. Cm, Cambrian; O, Ordovician; S, Silurian; D, Devonian; C, Carboniferous; P, Permian; Tr, Triassic; J, Jurassic; K, Cretaceous; T, Tertiary.

[1]Department of Geology, University of Cincinnati, Post Office Box 210013, Cincinnati, OH 45221–0013, USA. [2]Department of the Geophysical Sciences, University of Chicago, 5734 South Ellis Avenue, Chicago, IL 60637, USA.

*To whom correspondence should be addressed. E-mail: arnold.miller@uc.edu

The results (Fig. 1C) demonstrate that the initial set of maxima is maintained, although the relative heights of some maxima were altered and, interestingly, an additional maximum is observed for the Late Guadalupian interval of the Late Permian. Second, to investigate the possibility that the means of observed maxima were inflated by the presence of a small number of genera that persisted all the way to the Recent, the analysis was also conducted after culling from the original database all genera that are extant today. The resulting pattern was quite similar to that observed without culling (Fig. 1D), although the Hettangian maximum was reduced, and the Early Paleocene maximum is no longer statistically significant.

We have carried out the same analyses using several alternative protocols: the use of median cohort longevities rather than means; the use of stage-level bins rather than substages, which would have permitted the inclusion of genera from the database whose first or last occurrences were not resolved to substage; and the merging together of adjoining substage bins that were either of unusually short duration or contained small cohorts. Although the nature of some maxima changed—particularly the broadening of some postextinction maxima to include the mass extinctions that immediately preceded them—they did not appreciably alter the results reported here, demonstrating that the results are robust.

Figure 1 exhibits two additional features. First, the pattern is almost entirely limited to the post-Paleozoic. There is no indication of a meaningful pattern at any time before the Late Guadalupian, nor is there any consistent association between Paleozoic mean longevity patterns and the record of Paleozoic extinction (Fig. 1B). Given that the mean duration of Paleozoic substages was greater than that of the post-Paleozoic (15), there might be some concern that the depressed Paleozoic pattern is an artifact: A Paleo-

zoic genus that was extant for the same amount of absolute time as a post-Paleozoic genus might have been extant for a smaller number of substages. However, the actual differences in mean substage lengths between the two intervals [3.72 million years (My) for the Paleozoic versus 3.36 My for the post-Paleozoic] are too small to have caused the longevity differences observed here. Rather, the pattern bolsters the growing evidence suggesting that there were differences in the dynamics of Paleozoic versus post-Paleozoic origination and extinction (19), with the transition perhaps triggered by the Late Permian mass extinction. In addition, preserved biotas came predominantly from epicontinental seas in the Paleozoic but from open ocean environments in the post-Paleozoic (20). This may have caused a secular transition in the evolutionary attributes of marine taxa, given indications that the dynamics of taxa differed noticeably between these two settings (21).

Second, in two cases, the maxima include cohorts that originated in substages during intervals of mass extinction. The peak value observed in the Hettangian was immediately preceded by a value that was nearly as high in the Late Norian, an interval of mass extinction (Fig. 1B). In addition, the Late Guadalupian peak that emerged when genera that became extinct during mass extinctions were culled from the data (Fig. 1C) occurred in an interval of elevated extinction that preceded the end-Permian coup de grace (22). Thus, in at least some instances, it appears that genera originating during intervals of elevated extinction that survived these events had longevities, and perhaps other characteristics, comparable to those observed in recovery cohorts. This result is not unexpected, given previous analyses of "disaster taxa" that survived mass extinctions (1–5, 10).

One possible mechanism for the results documented here concerns the effect of species-level origination and extinction rates on the longevities of genera. If, as would be expected, speciation rates are high relative to species extinction rates in the aftermaths of mass extinctions, then a genus that originates shortly after an extinction event, or carries over from before the event, will tend to accumulate species during the substage after the event. All else being equal, this initially higher species richness should enhance the longevity of the genus relative to genera that originate after the interval of elevated speciation rates. To illustrate this mechanism, Fig. 2 shows results from a basic birth-death model (15, 23, 24). Speciation rates within genera are assumed to be higher than species extinction rates for an initial substage; afterward, speciation and extinction rates are assumed equal.

These calculations suggest that a substantial difference in median genus longevity can result from a modest and short-lived excess of speciation over species extinction. For example, the average long-term rate of species extinction of marine invertebrates is in the neighborhood of

0.25 per lineage-million-years (25). In this case, a speciation rate that is 60% higher than extinction for just a few million years, after which it is equal to extinction, will increase median genus duration by ~50% relative to a speciation rate that is equal to extinction from the start.

Although our analyses confirm expectations that several recovery cohorts had greater mean longevities than did cohorts originating at other times, they do not demonstrate that these same genera also had unusually large geographic or environmental ranges. This can only be determined by directly evaluating the spatial occurrences of these genera in strata around the world.

Our findings also have ramifications for conservation biology. There is compelling evidence that the earth is currently in the midst of a human-induced mass extinction (26) and that many of the survivors of this extinction are likely to be ecological generalists capable of subsisting in a wide spectrum of settings. The present analysis suggests that the same will be true of any initial recovery of global biodiversity from this extinction and that the taxa that contribute to the recovery are likely therefore to persist for extended periods into the future.

References and Notes
1. J. K. Schubert, D. J. Bottjer, *Geology* **20**, 883 (1992).
2. D. L. Rodland, D. J. Bottjer, *Palaios* **16**, 95 (2001).
3. M. L. Droser, D. J. Bottjer, P. M. Sheehan, G. R. McGhee, *Geology* **28**, 675 (2000).
4. D. H. Erwin, *Proc. Natl. Acad. Sci. U.S.A.* **98**, 5399 (2001).
5. P. M. Sheehan, *Ann. Rev. Earth. Planet. Sci.* **29**, 331 (2001).
6. D. H. Erwin, *Science* **279**, 1324 (1998).
7. D. Jablonski, *Science* **279**, 1327 (1998).
8. J. W. Kirchner, A Weil, *Nature* **404**, 177 (2000).
9. J. W. Kirchner, *Nature* **415**, 65 (2002).
10. D. H. Erwin, *Trends. Ecol. Evol.* **13**, 344 (1998).
11. D. Jablonski, *Science* **231**, 129 (1986).
12. D. Jablonski, *Science* **253**, 754 (1991).
13. J. J. Sepkoski Jr., *Bull. Am. Paleontol.* **363**, 1 (2002).
14. J. M. Adrain, S. R. Westrop, *Science* **289**, 110 (2000).
15. Materials and methods are available as supporting material on *Science* Online.
16. A similar pattern was derived independently by A. V. Markov (27), but was discussed in a different context from that of the present study.
17. M. Foote, *Paleobiology* (suppl.) **26**, 74.
18. D. M. Raup, J. J. Sepkoski Jr., *Science* **231**, 833 (1986).
19. M. Foote, *Paleobiology* **26**, 578 (2000).
20. L. J. Walker, B. H. Wilkinson, L. C. Ivany, *J. Geol.* **110**, 75 (2002).
21. P. M. Sheehan, *Paleobiology* **1**, 205 (1975).
22. S. M. Stanley, X. Yang, *Science* **266**, 1340 (1994).
23. D. G. Kendall, *Ann. Math. Statist.* **19**, 1 (1948).
24. D. M. Raup, *Paleobiology* **11**, 42 (1985).
25. D. M. Raup, *Paleobiology* **17**, 37 (1991).
26. N. H. Myers, A. H. Knoll, *Proc. Natl. Acad. Sci. U.S.A.* **98**, 5389 (2001).
27. A. V. Markov, *Paleontol. J.* **36**, 121 (2002).
28. We thank D. M. Raup and D. H. Erwin for discussions, A. Hendy for technical assistance with the figures, and NASA (Program in Exobiology) and NSF (Programs in Biocomplexity and in Geology and Paleontology) for financial support. This is Paleobiology Database Publication No. 20.
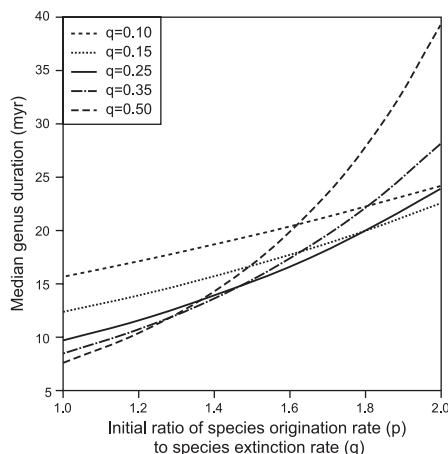
Fig. 2. Elevation in median genus duration produced during an interval in which speciation rate (*p*) within the genus exceeds species extinction rate (*q*). The initial interval is assumed to be 4 My, about the length of a substage in our analysis.